Colloid Polym Sci 276:81–86 (1998)

ORIGINAL CONTRIBUTION

H.B. Bohidar
S.S Jena
S. Maity
A. Saxena

Dielectric behaviour of Gelatin solutions and Gels

Received: 10 February 1997
Accepted: 2 September 1997

H.B. Bohidar (✉) · S. Jena · S. Maity
A. Saxena
Jawaharlal Nehru University
School of Physical Sciences
New Delhi - 110067
India

Abstract Sol and Gel state properties of aqueous gelatin solutions of concentrations 4%, 6%, 8% and 10% (w/v) have been investigated through dielectric relaxation studies done at various temperatures in the range $T = 20$–$60\,^{\circ}C$ carried out over a frequency range $f = 20$ Hz–10 MHz and no relaxation of any nature was observed. The sharp transition observed at the gelation temperature T_{gel} provided an excellent matching with the same measured through differential scanning calorimetry (DSC). The capacitance (C_p) values above $f = 100$ kHz became increasingly negative as the gel was melted to the sol state. However, in the gel state C_p was found to be almost independent of temperature for frequencies above 100 kHz. At frequencies lower than 10 kHz, C_p measured was $\sim 10^5$ F, implying pronounced interfacial polarization either due to electro-chemical reaction or because of ions getting trapped at some interface within the bulk.

Key words Gelatin – sol–gel – dielectric properties

Introduction

In our earlier works, we have reported a detailed light scattering study on the kinetics of sol–gel transition in gelatin [1]. The phase diagram in this work was established through differential scanning calorimetry experiments. We have established the existence of three distinct domains in these phase diagrams corresponding to the sol state-I where the chains have random coil conformations, sol-II where single and triple helices begin to form and the gel state where the triple helices get intertwined physically to form a giant interconnected three-dimensional structure. We have also observed spinodal line in this system through laser light scattering techniques [2] and the results were interpreted through Tanaka's mean field theory of density fluctuation in gels [3, 4].

Gelatin, which is denatured collagen, undergoes thermoreversible gelation in hydrogen-bond friendly environment, when the protein concentration is higher than typically 2–3% (w/v). A lot of effort has been devoted in the past to study the kinetics of gelation mechanism of this protein [5–11]. Considering the fact that this is one of the most abundantly found protein in mammals and its wide use in food, pharmaceutical and cosmetic industries, the importance of such studies can be hardly stressed. Dielectric relaxation method is a powerful technique to investigate the structure of free bulk water and that bound to the polymer networks and gels. The typical relaxation behavior of a dielectric material is shown in Fig. 1. The real part of the dielectric constant $\varepsilon'(f)$ exhibits an initial plateau region that defines the zero-frequency dielectric constant ε_0 followed by a relaxing part in the intermediate frequency domain which levels off at $f \to \infty$ to $\varepsilon_\infty = n_D^2$, where n_D is the refractive index of the bulk. The imaginary part $\varepsilon''(f)$, on the other hand, has a bell-shaped structure and the frequency value corresponding to the maximum $\varepsilon''(f)$ defines the average relaxation time of the dipoles in

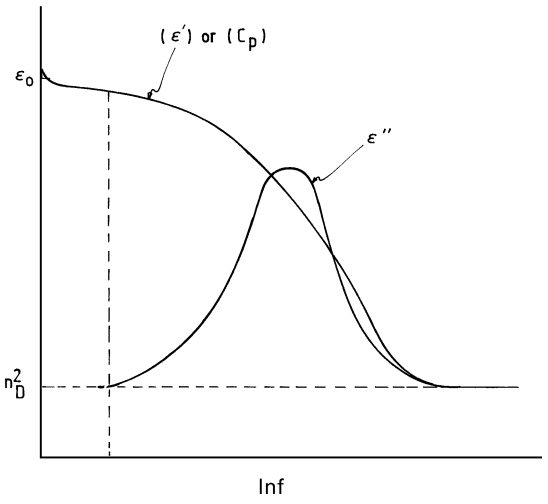

Fig. 1 The frequency spectrum of $\varepsilon'(f)$ and $\varepsilon''(f)$ of a typical dielectric material. The horizontal line corresponds to $\varepsilon'(f)$ at $f = \infty$ and equals n_D^2 where n_D is the refractive index of the material. The vertical dotted line defines the frequency window (20 Hz $\leqslant f \leqslant$ 10 MHz) probed by our instrument

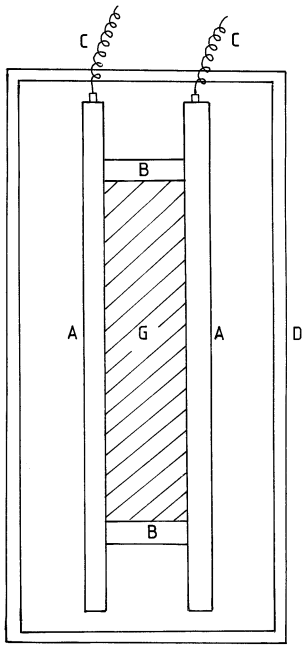

Fig. 2 Diagram of the dielectric cell (not to scale). A: electrodes (size = 40 mm × 30 mm × 0.25 mm), experiments were performed with platinum, gold and copper electrodes; B: Teflon spacers (size = 3 mm^3); C: electrode connecting leads to the LCR bridge; G: sample chamber and D: was the insulated double-walled housing for temperature control. Temperature was regulated by a circulating water bath and monitored at the top and the bottom of the cell by calibrated thermocouples to avoid thermal gradients in the sample

the bulk material. The width of $\varepsilon''(f)$ profile is dependent on the dipole relaxation time distribution of the material. Further details on this can be obtained from ref. [12].

In the present work, we have subjected the gelatin samples to dielectric relaxation measurements and have observed interesting behavior both in the sol and gel states. These results have been correlated with our earlier data on gelatin. The objective was to see any possible change in the zero-frequency dielectric constant ε_0 at the sol–gel transition point and, hence, to deduce the fraction of water that is bound to the gel network. In addition, we attempted to locate the signature of Debye viscosity relaxation (if any) in this system. And to the best of our knowledge, the dielectric relaxation results for this sample have not been reported hitherto.

Materials and methods

Details of sample preparation have been described else where [1]. The protein concentrations were 4%, 6%, 8% and 10% w/v of the solvent. The dielectric relaxation experiments were carried out using a Hewlett–Packard 4284-A precision LCR meter (frequency range 20 Hz–10 MHz). A two-terminal parallel plate platinum electrode assembly was used, see Fig. 2 for a sketch of this cell. This prevents any possibility of reaction of the stock material with the electrode. Experiments were repeated with 0.2 mm thick Teflon-covered gold electrodes for the sake of comparison. The temperature controller was same as described in ref. [13]. The reported capacitance values pertain to the platinum electrode cell unless stated otherwise. The measured empty cell (C_o) and lead (C_L) capacitance values were $C_o = (3.08 \pm 0.02)$pF and $C_L = (2.03 \pm 0.01)$pF. The frequency window probed by our instrument is shown in Fig. 1. The experiments were carried out in two steps. First, the electrode cell was filled with the solvent without NaCl and measurements taken from 20 °C to 60 °C to calibrate the cell assembly. Figure 3 shows the measured capacitance C_p derived from the capacitance vs. frequency data. The measured C_P value is related to the real part of dielectric constant ε' at a given frequency as

$$\varepsilon'(f) = \frac{C_P(f) - C_L}{C_o} . \qquad (1)$$

Since, $C_p(f)$ was two-orders of magnitude greater than either C_o or C_L, in all our measurements $\varepsilon'(f) = C_p(f)/C_o$. The cell was calibrated from the 100 kHz data of C_p at 20 °C. The measured C_p was 242 pF (Fig. 3) and C_p is related to the dielectric constant of bulk material (water in our case) as

$$C_P = C_o \times \varepsilon + C_L , \qquad (2)$$

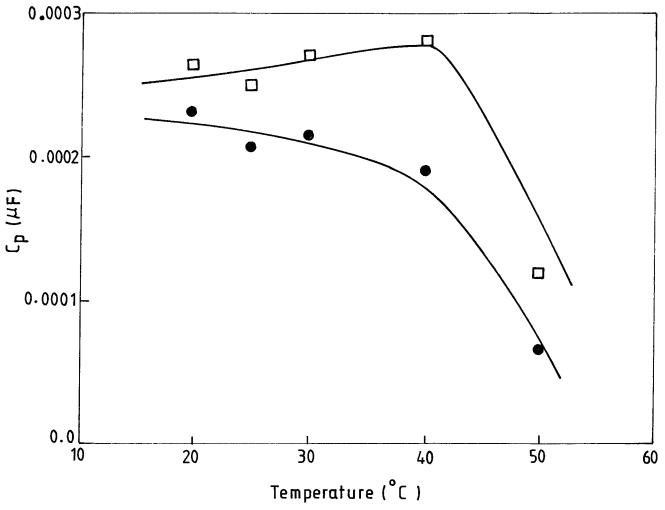

Fig. 3 Response of the cell filled with the solvent at frequencies 0·01 MHz (□) and 0.1 MHz (●) at various temperatures. There was no NaCl in the solvent. Calculation gives $\varepsilon' = 80$ expected of pure water at 20 °C. Size of the symbols designate typical error bars in the data points

using our measured values of $C_o = (3.086 \pm 0.06)$pF and $C_L = (2.03 \pm 0.01)$pF, values of ε_{H_2O} obtained was approximately 80 providing an excellent match to the standard value. The temperature profile of C_P vs. 1/T at 100 kHz could be fitted to a linear relation expected of pure water behavior. Further discussions on this are available elsewhere [14]. The $C_p(f)$ or $\varepsilon'(f)$ vs. f was measured to be a straight-line parallel to frequency axis with a constant value $\varepsilon' = (2.49 \pm 0.01)$ for Teflon. Hence, Teflon-coated electrodes of gold and copper had no dispersive artifact on experimental data. In the second step, the gelatin samples of various concentrations were loaded into the dielectric cell and experiments repeated with copper, gold and platinum electrodes.

Theoretical background

The following elucidates the principle of dielectric relaxation experiment. Electric polarizability and relaxation times of molecules or side chains are normally probed through this technique. While the polarizability essentially quantifies the electric dipole moment suitably averaged over the entire configurational space, the physical dimension of the molecules or side chains manifest themselves in the relaxation time measurements. These two dielectric parameters are not necessarily related to each other, nonetheless, the combination of these two can be very powerful in the measurement of macromolecular structure. The electric polarization P comprises of two parts namely, the atomic and electronic polarizability P_∞ and the orientational polarization of the electric dipole P_{dip}, hence [14],

$$P = P_\infty + P_{dip}\,, \tag{3}$$

when the field is switched on, P_∞ appears instantaneously but P_{dip} takes a finite time more or less increasing in an exponential fashion to a saturation value. It is possible to get an insight into P_{dip} by measuring the frequency-dependent profile of complex dielectric constant, $\varepsilon(f) = \varepsilon'(f) - i\varepsilon''(f)$. Designating the zero frequency and infinite frequency dielectric constants as ε_o and ε_∞, the frequency dependence (f) of ε can be written in the familiar Debye equation as

$$\varepsilon(f) = \varepsilon_\infty + \frac{\varepsilon_o - \varepsilon_\infty}{1 + i\omega\tau}\,, \tag{4}$$

where τ is the relaxation time of the dipoles. From this expression, one can compute $\varepsilon'(f)$ and $\varepsilon''(f)$ and plot the dispersion behavior as depicted in Fig. 1.

Debye interpreted the relaxation time τ at absolute temperature in terms of the rotation of the polar molecules in a continuum medium with friction and using Stokes law for rotation of an equivalent sphere of radius a, τ comes out as [12]

$$\tau = \frac{f}{k_B T} = \frac{8\pi\eta a^3}{k_B T}\,, \tag{5}$$

where the rotational frictional coefficient $f = 8\pi\eta a^3$ and k_B is the Boltzmann constant. Normally, in long-chain polymers one has to take into account a distribution of relaxation times originating from molecular interactions, variations in the lengths of side chains and groups, etc. These effects are accounted for in the relaxation time distribution function. This often results in the flattening of the $\varepsilon''(f)$ dispersion profile.

Results and discussion

The typical dispersion behavior of the measured capacitance C_p below and above gelation temperature is shown in Fig. 4. For all the concentrations of gelatin the curves more or less looked qualitatively similar. The curves-I are for samples without NaCl and II are with NaCl present in the system. Two features are clear from these data. When NaCl was added C_P values got enhanced by a factor of 2. Secondly, as the gelation temperature approached C_P values at a given frequency showed gradual decrease. A typical situation is shown in Fig. 5. At the T_{gel} point there was a sharp fall in the C_p value indicating a thermodynamic transition. Below this, the C_p values remained

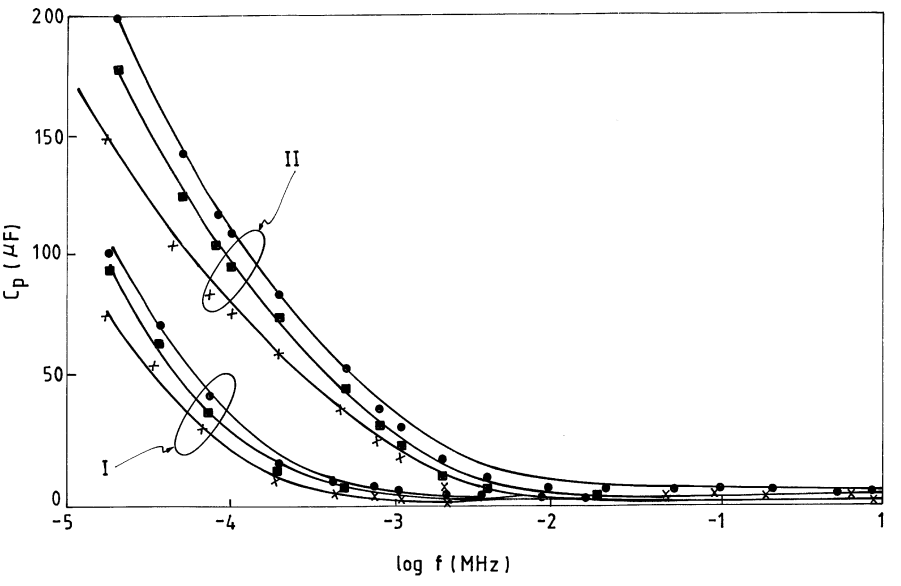

Fig. 4 The measured capacitance (C_p) of a 10% (w/v) sample of gelatin in the sol and gel states as function of frequency with (set-II) and without (set-I) 0.01 M NaCl being present in the sample. Symbols: (●), (■) and (★) correspond to sols at 60 °C and 40 °C and gels at 25 °C. Size of the symbols designate typical error bars in the data points

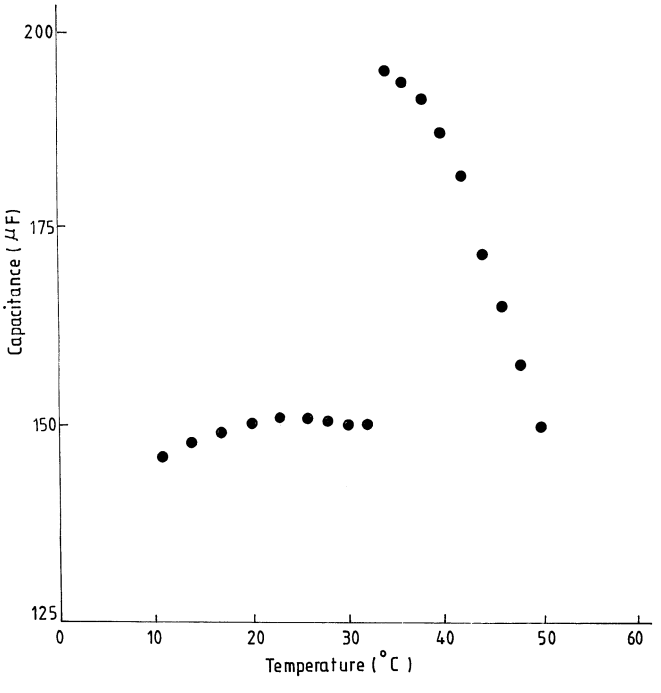

Fig. 5 Transition in capacitance at gelatin temperature T_{gel} for a 10% (w/v) sample with 0.1 M NaCl as the system evolves to a gel state ($T_{gel} = 30°$). The transition temperature provides excellent matching with the value measured through differential scanning calorimetry (see Table I) ($f = 10$ kHz). Size of the symbols designate typical error bars in the data points

almost same whereas above T_{gel} it decreased continuously as the temperature was raised to 60 °C.

Table 1 shows the gel transition temperatures T_{gel} measured from DRE studies and the corresponding values

Table 1 Jump in capacitance values (ΔC_p) as the system evolves from sol to gel-state, T_{gel} were measured from DRE and DSC data. The measured gel state capacitance values at 20 °C of 10%, 8%, 6% and 4% (w/v) samples with 0.01 M NaCl were (160 ± 5) μF, (120 ± 5) μF, (90 ± 3) μF and (75 ± 3) μF, respectively. $\Delta C_p = (C_p)_{sol} - (C_p)_{gel}$ at the gel transition point T_{gel}

Concentration C% [w/v]	ΔC_p [μF]	T_{gel}[K] [DRE]	T_{gel}[K] [DSC]
4	16 ± 1	297 ± 2	298 ± 0.5
6	22 ± 1	299 ± 2	300 ± 0.5
8	33 ± 2	304 ± 2	302 ± 0.5
10	40 ± 2	306 ± 2	303 ± 0.5

obtained earlier from differential scanning calorimetric studies. The magnitude of jump in the capacitance values (ΔC_p) as the gel point was approached from above T_{gel} varied from one concentration to another and this is listed in Table 1. Figure 4 also indicates that all the significant dispersion behavior was contained in the low-frequency (< 100 kHz) domain of the spectrum. Hence, we have chosen the behavior of C_p at two distinct frequencies 10 kHz and 100 kHz obtained at different temperatures to differentiate between the high- and low-frequency features of the dielectric constant $\varepsilon'(f)$. Figure 6 shows the variation of $C_p(f)$ as the gel point was approached. Here again at 10 kHz C_p showed a jump to a higher value close to T_{gel} and no such behavior could be observed at 100 kHz. Infact at this frequency, C_p showed negative values that increased in magnitude with temperature gradually. This was observed for samples of all concentrations from 4% to 10% (w/v) of gelatin. The size of the jump in C_p value was smaller in samples not containing NaCl compared to those with NaCl. At lower concentrations of gelatin this was

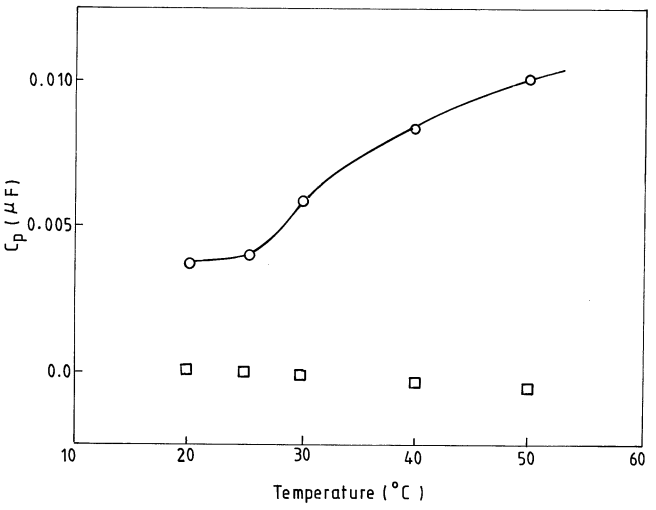

Fig. 6 The variation of C_p versus temperature for a 10% (w/v) sol of gelatin without any added salt as the system evolves to the gel state at two selected frequencies 10 kHz (○) and 100 kHz (□). Notice the small jump in C_p value at T_{gel} because no NaCl was present. Size of the symbols designate typical error bars in the data points

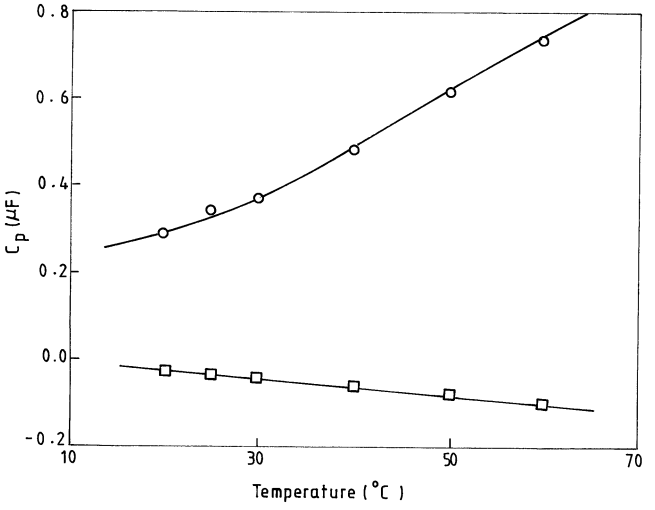

Fig. 7 The sample was same as in Fig. 6 but with 0.1 M NaCl present in the solution. Compared to the C_p values reported in Fig. 6, in this sample the capacitance got enhanced almost by 100 times at $f = 10$ kHz (○) but at $f = 100$ kHz (□) these almost remained same as in Fig. 6. Size of the symbols designate typical error bars in the data points

even less pronounced. Nonetheless, the negative capacitance feature remained at the frequencies above 100 kHz.

The behavior of negative capacitance was observed in all samples as the electrode material was changed from platinum to gold to copper increasing in magnitude in that order. In addition, the last two electrodes showed visible decoloration of the electrode surface implying possible chemical reaction with the electrode material. This behavior was more pronounced when NaCl was present in the solution (Fig. 7) indicating that possibly C_p values did not reveal the bulk dielectric behavior of the material. The fact that this behavior got enhanced at higher temperatures and higher frequencies implied that the experiments basically probed ionic mobility of free ions in the sol and gel states of gelatin. On the low-frequency side (<10 kHz), the value of C_p and hence ε', was observed to be (Figs. 6 and 7) of the order of 10^5 F which was too high. This can be attributed to the pronounced interfacial polarization either due to electrochemical reaction or due to ions getting trapped at some interface within the bulk. Similar features have been observed earlier in the case of a variety of physical situations [14].

The objective in these studies had been twofold. First, to see if there was any relaxation process within the frequency range 20 Hz–10 MHz and secondly, to probe the quantum of water molecules bound to the interstatial space inside the gel network. We did not observe any relaxation behavior of any kind upto a frequency of 10 MHz. Using Debye viscosity relaxation equation, (Eq. (5)) and using the literature data [1] one finds that in sol state, the radius of gyration of gelatin chain R_g, varies between 19 and 28 nm, this would imply that one would see a relax ation peak in the typical frequency range of 1.5–5 kHz. This was not observed in any of our samples. As far as the second objective was concerned, the data did show a step-like change at T_{gel} in C_p vs. temperature plot (Fig. 5). This is typical of a first-order phase transition. The T_{gel} values provide excellent matching with the data obtained from DSC measurements. Capacitance (hence ε') values showed very high values below 10 kHz that increased with temperature, gelatin concentration and presence of NaCl. Above 100 kHz, the measured capacitance was found to be negative and its magnitude increased with temperature and gelatin concentration. Jonscher has proposed several physical models to explain the origin of negative capacitance [14, 15].

The change in ΔC_p at transition temperature provides an indication of the amount of unfreezing of the dipolar part of the gel during the onset of gelation. This can perhaps be related to the water content of the gel network. Since, water is a strongly polar molecule, one would see the dominance of this in C_p measurement. In our measurements, we have found contribution from ionic conduction on lower frequency (<100 kHz) side of measurements. However, at frequencies above 100 kHz upto 10 MHz, the dielectric constant was noticed to be independent of the frequency, which we believe to be that of the bulk sample in our above analysis (Fig. 4). Lack of relevant experimental data in the literature did not allow us to provide any comparison. Further investigations of this system at microwave frequencies is likely to improve the understanding of the origin of this behavior.

References

1. Bohidar HB, Jena SS (1993) J Chem Phys 98: 8970–8977; ibid (1994) J Chem Phys 100: 6888–6895
2. Bohidar HB, Jena SS (1993) J Chem Phys 98: 3568–5670
3. Tanaka T, Hocker LO, Benedek GB (1973) J Chem Phys 59: 5151–5159
4. Tanaka T, Ishiwata S, Ishimoto C (1977) Phys Rev Lett 38: 771–774
5. Ren SZ, Shi WF, Zhang UB, Sorensen CM (1991) Phys Rev A 45: 2416–2422
6. Djabourov M, Leblond J, Papon P (1988) J Phys (Paris) 44: 319–332; ibid 333–343
7. Pezron I, Herning T, Djabourov M, Leblond J (1990) In: Burchard W, Ross-Murphy SB (eds) Physical Network Polymers and Gels. Elsevier Applied Sciences, London, 231–254
8. Herning T, Djabourov M, Leblond J, Takekart G (1991) Polymer 32: 3211–3217
9. Pezron I, Djabourov M, Leblond J (1991) Polymer 32: 3201–3210
10. Busnel JP, Morris ER, Ross-Murphy SB (1989) Int J Biol Macromol 11: 119–125
11. Busnel JP, Ross-Murphy SB (1988) Int J Biol Macromol 10: 121–124
12. Takashima S (1969) In: Leach SJ (eds) Physical Principles and Techniques of Protein Chemistry-part-A. Academic Press, New York, 291–367
13. Bohidar HB, Berland T, Jossang T, Feder J (1987) Rev Sci Instr 58: 1422–1426
14. Jonscher AK (1986) J Chem Soc Faraday Trans-II 82: 75–81
15. Jonscher AK (1997) Universal Relaxation Law. Chelsea Dielectric Press, London